ENCIT 2018

ABCM Associação Brasileira de Engenharia e Ciências Mecânicas

17th Brazilian Congress of Thermal Sciences and Engineering
November 25th-28th, 2018, Águas de Lindóia, SP, Brazil

ENCIT-2018-0189
NUMERICAL SIMULATIONS OF THERMOMAGNETIC CONVECTION INSIDE A THIN CAVITY

Ciro Fraga Alegretti*
Universidade Estadual de Campinas, Faculdade de Engenharia Mecânica, Departamento de Energia, Rua Mendeleyev, 200, Unicamp, 13083-970, Campinas-SP, Brazil
ciro.alegretti@gmail.com

Arthur Alves Rios Campos*
Francisco Ricardo Cunha*
Universidade de Brasilia, Departamento de Engenharia Mecânica, Campus Universitario Darcy Ribeiro, UnB, 70910-900, Brasilia-DF, Brazil
72campos@gmail.com, frcunha@unb.br

Rafael Gabler Gontijo*
Universidade Estadual de Campinas, Faculdade de Engenharia Mecânica, Departamento de Energia, Rua Mendeleyev, 200, Unicamp, 13083-970, Campinas-SP, Brazil
rafaelgabler@gmail.com

*Vortex Group - Fluid Mechanics of Complex Flows

Abstract.
This paper is focused on the theoretical and numerical investigation of the natural convection of a ferrofluid in a two dimensional cavity. This physical problem consists in a coupling between hydrodynamic, magnetic and thermal phenomena. The latest formulation for the Maxwell stress tensor and the superparamagnetic regime are considered. A scaling analysis is presented, which indicates the ideal aspect ratio for the rectangular cavity. Constant temperature condition is considered for the side walls, whereas adiabatic for the bottom and top walls. The Finite Differences Method is applied to the partial differential equations discretization. The semi-implicit fractional-step scheme is implemented to a staggered grid in order to solve the coupled equation system. Code validation is conduced in respect to previous studies of natural convection in the absence of magnetic effects. A non-uniform magnetic field is applied to the cavity. The enhancement of heat transfer properties are presented both qualitatively and quantitatively. Flow pattern and temperature fields illustrate the attenuation of temperature gradients under magnetic field application.

Keywords: *ferrofluid, thermomagnetic convection, superparamagnetism*

1. INTRODUCTION

Ferrofluids are colloidal suspensions of magnetic particles in a carrier medium, which thermophysical properties are strongly disturbed under magnetic field influence (Rosensweig, 2013). The solid magnetic suspended particles, of nanometric scale and reduced from a ferromagnetic solid, are coated with a dispersant layer and are subjected to brownian motion, driven by the thermal agitation of the liquid matrix. As result, such colloidal suspensions are guarded against particle agglomeration and sedimentation (Ivanov and Kuznetsova, 2001), and so are energetically stable for a wide specter of physical conditions (Katharina and Kerstin, 2015).

Due to its colloidal composition, the suspended magnetic particles orientation are strongly influenced by the external magnetic field. Such interaction occurs via magnetic field forces and inner torques acting on the suspended particles, resulting in a very distinguish behavior. The interaction between ferromagnetic-based colloidal suspensions and magnetic fields is the object of study of Ferrohydrodynamics. Due to such response to an external field, novel applications have being conceived in different research fields in the past decade. Biocompatible ferrofluids are employed both on the separation and manipulation of microparticles and live cells, resulting in a low-cost and highly efficient method (Kose *et al.*, 2009), as efficient contrast agents in magnetic resonance imaging (Casula *et al.*, 2011). Moreover, ferrofluids enables the development of compact, quickly responsive, energetically efficient and electronically controllable adaptive lenses (Cheng *et al.*, 2011). In addition, water-based ferrofluid coolant provided an 50% improvement on the overall thermal efficiency in photovoltaic thermal units due to alternating magnetic field (Ghadiri *et al.*, 2015).

In a general matter, Ferrohydrodynamics problems comprehends the coupling between hydrodynamics and magnetics, given by velocity fields and the global magnetization of a ferrofluid, respectively. The global magnetization consists of a continuum approach to the volumetric average of the particles magnetic dipoles orientation (i.e.: the local magnetization in a nanometric scale inside a continuum volume), which is in constant balance with the flow. The complexity inherent to the physical interpretation and the mathematical modeling in Ferrohydrodynamics, which remains without a consolidated formulation, is carried out in several theoretical, numerical and experimental investigations (Shliomis, 2001; Odenbach and Müller, 2005; Cunha *et al.*, 2013).

Flow vorticity tends to misalign the magnetic dipoles of the suspended particles in respect to the external field orientation, resulting in a torque balance. In this study, a superparamagnetic regime will be considered, which represents the physical model where flow time scales are much greater than magnetic relaxation time scales. As result, the magnetic dipoles of the suspended particles are instantly restored to the external field orientation and the flow is not capable of disturbing the global magnetization, which remains aligned to the external magnetic field.

Natural convection flows in enclosures have been extensively investigated in the past decades for a wide range of aspect ratios, theoretical formulations and numerical methods (Ostrach, 1988). Laminar natural convection studies are strongly motivated by practical engineering problems, such as the cooling of nuclear reactors (Zitek and Valenta, 2014), electronic devices (Bessaih and Kadja, 2000) and photovoltaic applications (Fossa *et al.*, 2008). Due to the severity of the working conditions in some applications, an enhancement of heat transfer coefficients is required and can be achieved by the employment of nanofluids (Oztop and Abu-Nada, 2008), liquid metals (Viskanta *et al.*, 1986) and ferrofluids (Sheikholeslami and Gorji-Bandpy, 2014) as working fluid. In a general matter, the phenomena of natural convection subjected to external magnetic fields interaction is referred as *thermomagnetic convection*. Such branch is substantially different when investigated under the framework of Ferrohydrodynamics (FHD) or Magnetohydrodynamics (MHD). MHD and FHD thermomagnetic convection represents the coupling between buoyancy driven flows and magnetic fields, given by body forces and internal torques, respectively. In this study the laminar thermomagnetic convection in a square cavity will be investigated in a FHD formulation.

2. METHODOLOGY

2.1 Computational domain

The present study in conduced based on previous theoretical investigations regarding the thermomagnetic convection in cavities. Scaling analysis have shown, that for a narrow cavity with height ℓ and width δ_C, if $\ell \gg \delta_C$ the magnetic forces are balanced only by viscous forces (Cunha *et al.*, 2007). Therefore, the adopted geometry in this study is presented in Fig 1.

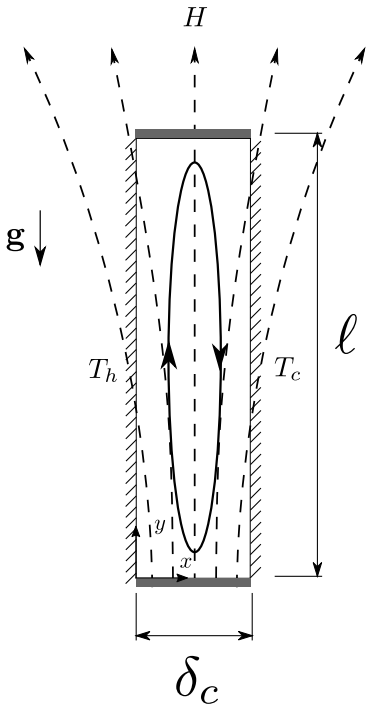

Figure 1. Narrow cavity geometry filled with superparamagnetic ferrofluid and subjected to an external field **H** and to gravitational acceleration **g**. Vertical walls are heated with constant temperatures (T_h and T_c) and horizontal walls are insulated.

2.2 Governing equations

Given the constant and different temperatures condition applied to the vertical walls, the buoyancy driven flow is generated from temperature-induced density stratification in addition to the magnetic mechanisms. In order to compute the coupling between temperature diffusion and flow convection, the Energy Equation will be considered, which in the absence of internal heat generation and neglecting internal energy production due to shear and magnetic stresses is given by

$$\frac{\partial T}{\partial t} + \mathbf{u} \cdot \nabla T = \alpha \nabla^2 T, \tag{1}$$

where T denotes the temperature scalar field, $\mathbf{u}$ the vectorial two-dimensional velocity field and α the thermal diffusivity of the fluid. Considering the asymmetric part of the stress tensor for a ferrofluid, the linear momentum equation is given by

$$\rho \left(\frac{\partial \mathbf{u}}{\partial t} + \mathbf{u} \cdot \nabla \mathbf{u} \right) = -\nabla p + \eta \nabla^2 \mathbf{u} + \rho \mathbf{g} + \mu_0 \left[\nabla \times (\mathbf{M} \times \mathbf{H}) + \mathbf{M} \cdot \nabla \mathbf{H} \right], \tag{2}$$

being ρ the suspension density, p the modified pressure field, η the effective shear viscosity, μ_0 the magnetic permeability, $\mathbf{M}$ the global magnetization in a continuum scale and $\mathbf{H}$ the applied magnetic field.

The global magnetization, under superparamagnetic regime $\mathbf{M}$ remains aligned to the external field $\mathbf{H}$ and is given by

$$\mathbf{M} = \chi \mathbf{H}, \tag{3}$$

where $\chi = \chi(T)$ represent the magnetic susceptibility of the medium, which is for the presented problem, alongside to the density, a function only of the temperature. Therefore, being the vectorial fields $\mathbf{M}$ and $\mathbf{H}$ collinear, Eq. (2) can be manipulated and rewritten as

$$\rho \left(\frac{\partial \mathbf{u}}{\partial t} + \mathbf{u} \cdot \nabla \mathbf{u} \right) = -\nabla p + \eta \nabla^2 \mathbf{u} + \rho \mathbf{g} + \mu_0 \chi(T) \nabla \left(\frac{H^2}{2} \right). \tag{4}$$

Being both magnetic susceptibility and density variations small, when compared to its values in at a temperature reference T_0, such variables can be modeled as a function of the temperature given by

$$\rho(T) = \rho_0 + \left. \frac{d\rho}{dT} \right|_{T_0} \Delta T \tag{5}$$

and

$$\chi(T) = \chi_0 + \left. \frac{d\chi}{dT} \right|_{T_0} \Delta T, \tag{6}$$

as proposed by Cunha *et al.* (2007). In addition, from the Boussinesq approximation, the intensity of buoyancy and magnetic forces per unit volume acting on the flow are given by

$$\boldsymbol{f_b} = -\rho_0 \beta \Delta T \boldsymbol{g} \tag{7}$$

and

$$\boldsymbol{f_m} = -\mu_0 \chi_0 \beta_m \Delta T \nabla \left(\frac{H^2}{2} \right), \tag{8}$$

where $\Delta T = T - T_0$ represents temperature variations to the reference temperature T_0, $\beta = -(1/\rho_0) d\rho/dT$ and $\beta_m = -(1/\chi_0) d\chi/dT$ denotes the thermal expansion and the pyrometric coefficients, respectively. Incorporating the Boussinesq approximation to the linear momentum equation and defining $\mathcal{P}$ as the total pressure modified by gravitational and magnetic potentials, Eq. (4) can be written as

$$\rho \left(\frac{\partial \mathbf{u}}{\partial t} + \mathbf{u} \cdot \nabla \mathbf{u} \right) = -\nabla \mathcal{P} + \eta \nabla^2 \mathbf{u} - \rho_0 \beta \Delta T \mathbf{g} - \mu_0 \chi_0 \beta_m \Delta T \nabla \left(\frac{H^2}{2} \right), \tag{9}$$

where the modified pressure is given by

$$\mathcal{P} = p - [\rho \mathbf{g} \cdot \mathbf{x} + \mu_0 \chi H^2/2] \tag{10}$$

The dependency of χ_0 with respect to the applied field $\boldsymbol{H}$ is given in our model by the Langevin approximation for the equilibrium magnetization of dilute ferrofluids

$$\chi_0 = \frac{M_0}{H} = \frac{\mathcal{L}(\alpha)}{H}, \tag{11}$$

where $\mathcal{L}$ denotes the Langevin function given by

$$\mathcal{L}(\alpha) = \coth(\alpha) - \frac{1}{\alpha} \tag{12}$$

and α is a parameter that expresses the ratio between the magnetic field energy with respect to Brownian energy

$$\alpha = \frac{\mu_0 m H_0}{k_B T}, \tag{13}$$

where m represents the magnetic dipole intensity of the ferromagnetic suspended particles, k_B the Boltzmann constant and d the particle diameter. Due to the incompressibility condition the Continuity Equation is also considered and regarding the external field $\mathbf{H}$, we consider the analytical solution for the magnetic field produced by a square surface with side $2a$ (MacCaig, 1987).

2.3 Dimensionless equations

Based on a scaling analysis between magnetic and convective terms present in Eq. (9), characteristic scales are adopted in terms of $\Delta T = T_h - T_c$: $u = (\mu_0 \beta_m \Delta T H_0^2/\rho)^{1/2}\hat{u}$, $v = (\mu_0 \beta_m \Delta T H_0^2/\rho)^{1/2}\hat{v}$, $t = L/(\mu_0 \beta_m \Delta T H_0^2/\rho)^{1/2}\hat{t}$, $p = \mu_0 \beta_m \Delta T H_0^2 \hat{p}$ and $\theta = (T - T_c)/(T_h - T_c)$. As result, the linear momentum equation be written as

$$\frac{\partial \mathbf{u}}{\partial t} + \mathbf{u} \cdot \nabla \mathbf{u} = -\nabla \mathcal{P} + Ra_m^{-1/2} Pr \nabla^2 \mathbf{u} - \chi_0 \theta \nabla (H^2/2), \tag{14}$$

where $Ra_m = \mu_0 \beta_m \Delta T H_0^2 L^2/\alpha\nu$ denotes the magnetic Rayleigh dimensionless parameter and $Pr = \nu/\alpha$ represents the Prandtl number. Moreover, the dimensionless energy equation is given by

$$\frac{\partial \theta}{\partial t} + \mathbf{u} \cdot \nabla \theta = Ra_m^{-1/2} Pr^{-1/2} \nabla^2 \theta, \tag{15}$$

which alongside to the dimensionless Eq's (11, 12, 13) and a given external field H will constitute the governing equations system for this numerical investigation. The magnetic Rayleigh number consists in a ratio between a magnetic buoyancy force and a force originated from diffusive effects in non-isothermal convective flows. As result, in order to investigate the effects of magnetic forces on the flow and temperature distribution patterns, numerical simulations are performed for $Ra_m \geq 10^6$. The obtained results are presented and discussed on the following section.

2.4 Numerical method

The set of coupled partial differential equations was solved using the finite difference method. In particular, we utilized a semi-implicit Crank-Nicolson scheme for energy equation, and a fractional-step scheme for the momentum equations (Kim and Moin, 1985). Our domain was discretized into a staggered grid, as described by Harlow and Welch (1965). In addition, we allocated the values of Θ and H at the center of each cell. The simulation starts by solving the energy equation and proceeds with the solution of the momentum equations. This process is iterated until steady state, which is defined according to the following criterion

$$\epsilon = max \left| \frac{\Theta_{ij}^{n+1} - \Theta_{ij}^{n}}{\Theta_{ij}^{n}} \right| \leq 10^{-6}. \tag{16}$$

The variables Θ_{ij}^{n+1} and Θ_{ij}^{n} are the temperatures at $x = i\Delta xj$ and $y = j\Delta y$ after two subsequent time steps.

The numerical method was validated after comparing our results for natural convection in a square cavity with the previous works of de Vahl Davis (1983) and Ashouri *et al.* (2010). The criteria for comparison was the average Nusselt number at the hot wall. For this purpose, we used a 81×81 grid. Table 1 shows that our results are in agreement with previous results.

Table 1. Comparison of the average Nusselt number at the hot wall.

Reference	$Ra = 10^4$	$Ra = 10^5$
Present work	2.237	4.532
de Vahl Davis	2.243	4.419
Ashouri et al.	2.248	4.533

3. RESULTS

The present numerical investigation is performed for two different magnetic field orientations, being one generated from a magnetic source placed at the bottom, and the other placed on the left side of the cavity.

For both configurations, a zero distance between the magnet and the cavity wall is considered. The parameters on Tab. 2 are held constant on both numerical experiments, while the magnetic effects on the thermomagnetic convective flow are studied for different magnetic Rayleigh numbers.

Table 2. Typical physical and numerical parameters

Grid nodes	Pr	α	δ/l	$2a/l$
32×64	10.0	10.0	0.1	1.0

3.1 Simulation I: magnetic source at the bottom of the cavity

Temperature fields, isotherms, streamlines and local Nusselt number on the hot wall for different magnetic Rayleigh numbers are presented in figures (2), (3), (4) and (5) respectively. It is possible to observe that the presence of the magnet on the bottom of the cavity pulls down the streamlines without producing another recirculation region (no bifurcation). At the same time the magnetic field breaks the symmetry on the temperature distribution. This effect leads to an increase on the local Nusselt number through the hot wall. This increase is associated with the thermomagnetic effect, which is more prominent in the first third of the wall where magnetic field gradients are higher. Note that for the highest field we have a maximum Nusselt number of around 20 against 2 for the lower field, an increase of 900%. It's important to highlight that the buoyancy driven flow, by definition, is established at $Nu > 1$.

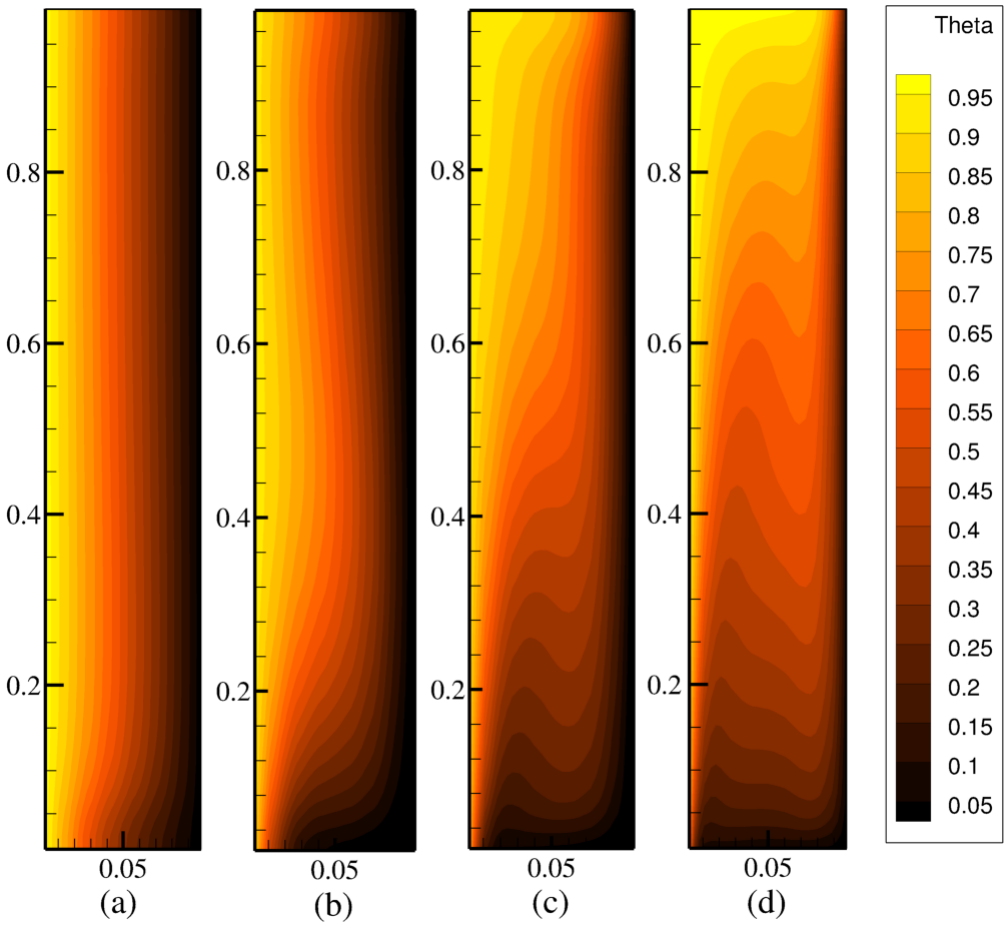

Figure 2. Temperature distribution inside the cavity for different magnetic Rayleigh numbers: (a) $Ra_m = 10^6$ (b) $Ra_m = 10^7$ (c) $Ra_m = 10^8$ (d) $Ra_m = 10^9$.

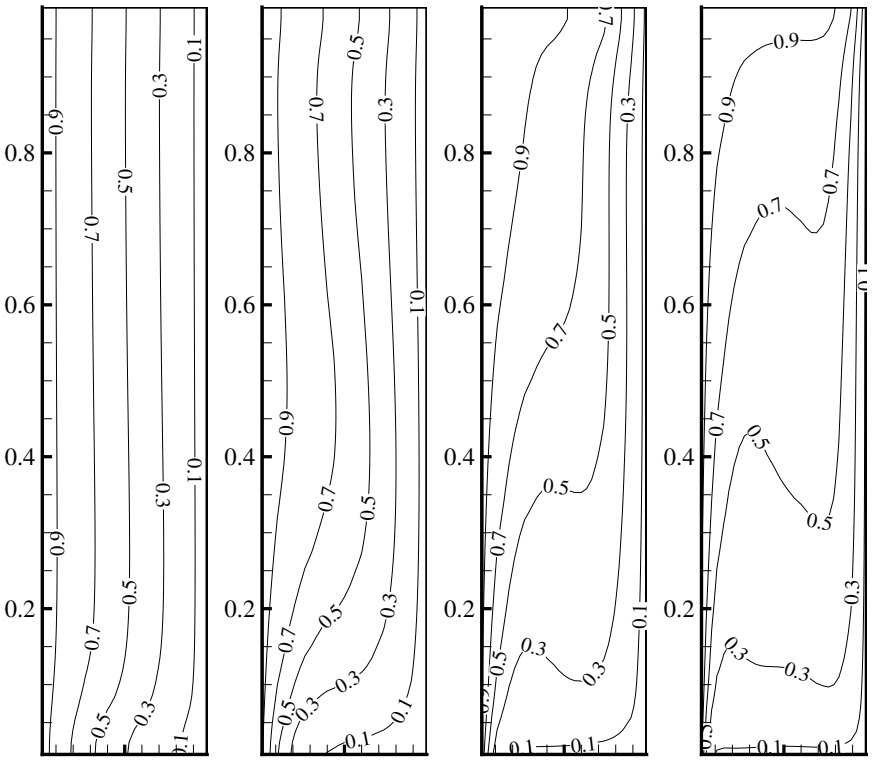

Figure 3. Temperature field contours inside the cavity for different magnetic Rayleigh numbers: (a) $Ra_m = 10^6$ (b) $Ra_m = 10^7$ (c) $Ra_m = 10^8$ (d) $Ra_m = 10^9$.

3.2 Simulation II: magnetic source on the side

Temperature fields, isotherms, streamlines and local Nusselt number on the hot wall for different magnetic Rayleigh numbers are presented in figures (6), (7), (8) and (9) respectively considering the new magnet configuration.

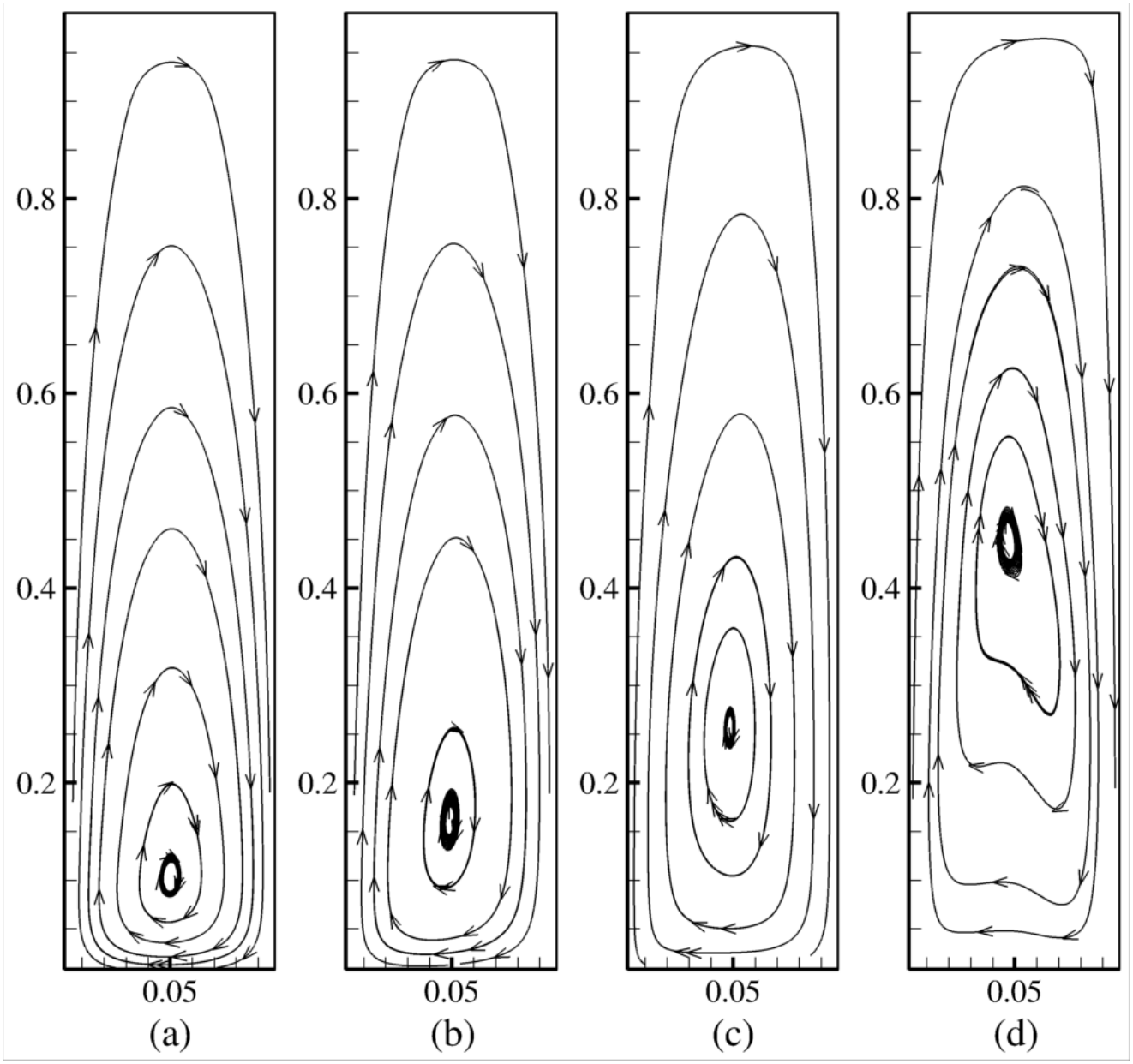

Figure 4. Streamlines inside the cavity for different magnetic Rayleigh numbers: (a) $Ra_m = 10^6$ (b) $Ra_m = 10^7$ (c) $Ra_m = 10^8$ (d) $Ra_m = 10^9$.

4. CONCLUSIONS

It is possible to notice that this field configuration is responsible for the appearance of two recirculating regions inside the cavity. This leads to a higher mixing and consequently to a higher increase in the local Nusselt number on the hot wall. Note that for the first configuration (magnet on the lower wall) the maximum local Nusselt number value was about 20, against 25 for this new configuration. A good explanation for this phenomenon lies on the vorticity equation for a superparamagnetic stratified fluid, which states that:

$$\frac{D\boldsymbol{\xi}}{Dt} = \xi \cdot \nabla \boldsymbol{v} + \frac{1}{\rho^2}\nabla\rho \times \nabla p + \nu\nabla^2\boldsymbol{\xi} + \mu_0 \nabla\chi \times \nabla\left(\frac{H^2}{2}\right), \tag{17}$$

where $\nu = \eta/\rho$ is the fluid's kinematic viscosity. Note that from Goldina et al. (2016) model, $\chi \sim T^{-1}$, so the production term due to magnetic effects in equation (17) is proportional to $-(\mu_0/T^2)\nabla\chi \times \nabla(H^2/2)$. Consequently, for a lateral magnetic field both $\nabla(H^2)$ and $\nabla\chi$ are collinear and horizontal at half cavity height and should result in no vorticity production, which is in agreement to our results due to the stagnation point at the streamtrace on the center line, where the Nusselt number reaches its maximum value. In addition, both the stagnation point location at the hot wall and the the flow topology provide a good correlation with figures (5) and (9), and explain the singularity in figure

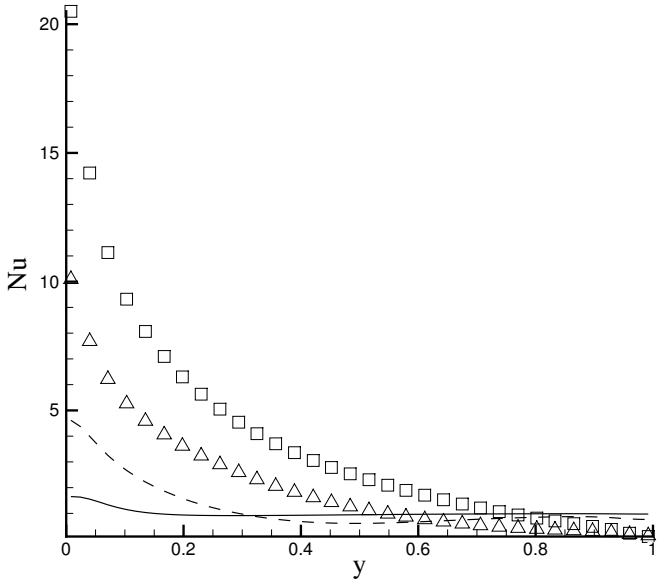

Figure 5. Local Nusselt number on the hot wall for different magnetic Rayleigh numbers. The solid line represents $Ra_m = 10^6$, dashed line $Ra_m = 10^7$, triangles $Ra_m = 10^8$ and squares $Ra_m = 10^9$.

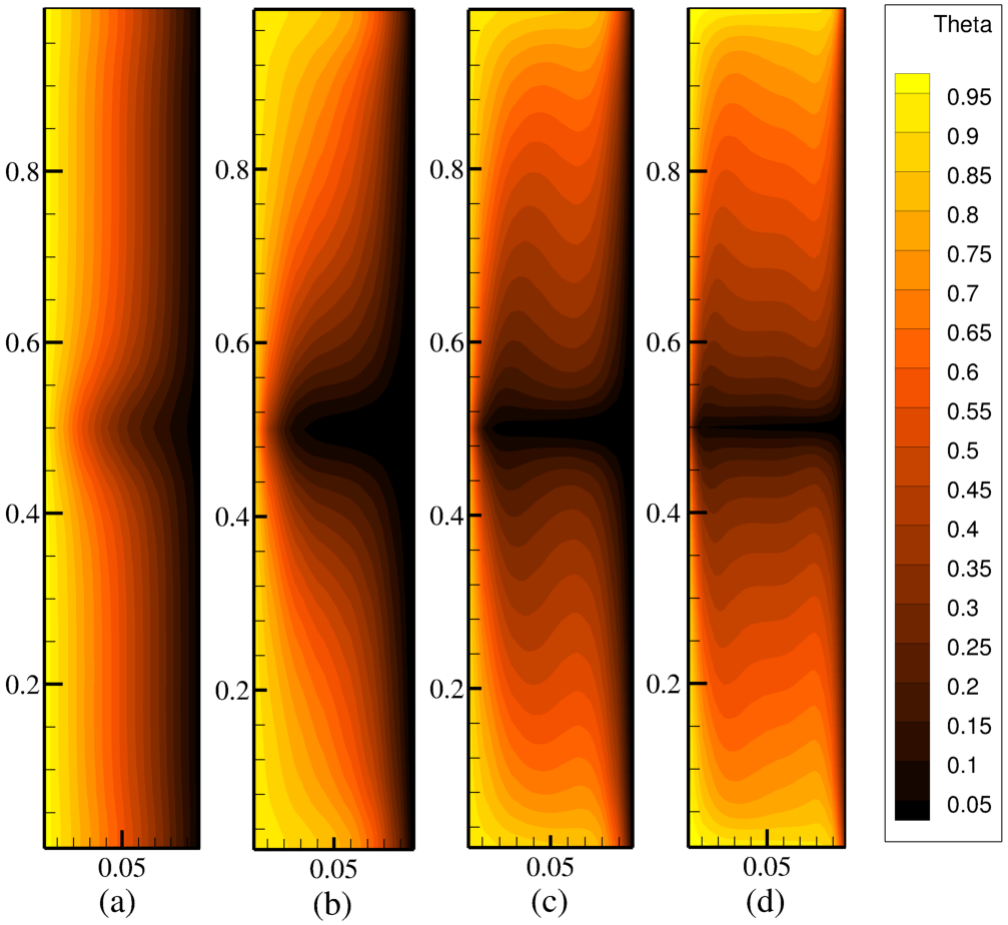

Figure 6. Temperature distribution inside the cavity for different magnetic Rayleigh numbers: (a) $Ra_m = 10^6$ (b) $Ra_m = 10^7$ (c) $Ra_m = 10^8$ (d) $Ra_m = 10^9$.

(9). In conclusion, the presence of two recirculating zones rotating in opposite directions leads to an enhancement in the transport of heat and momentum in the middle-cross section of the cavity.

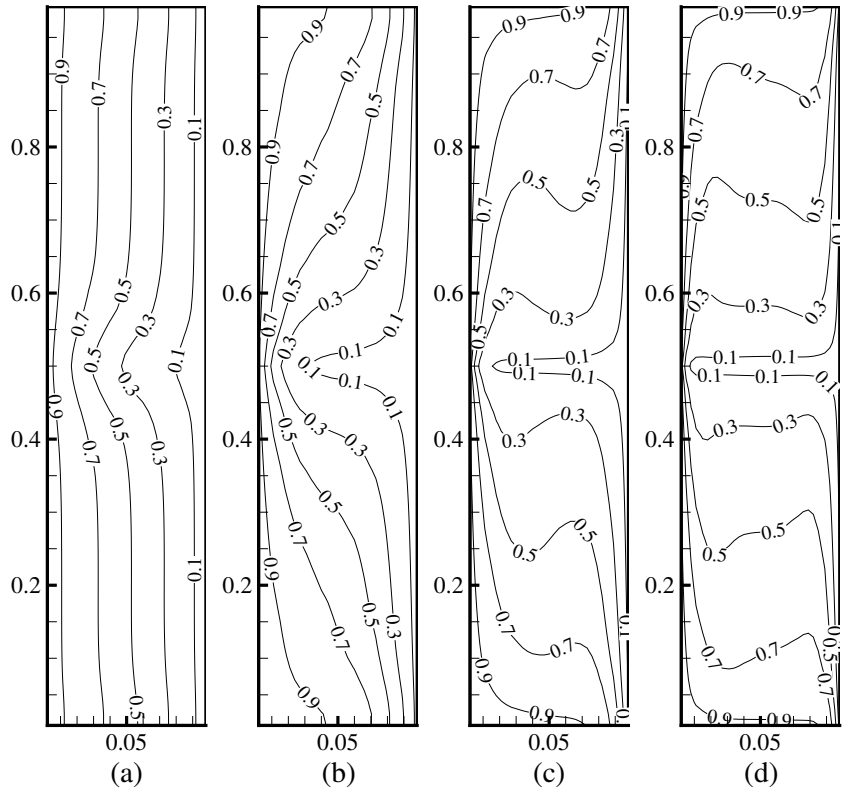

Figure 7. Temperature field contours inside the cavity for different magnetic Rayleigh numbers: (a) $Ra_m = 10^6$ (b) $Ra_m = 10^7$ (c) $Ra_m = 10^8$ (d) $Ra_m = 10^9$.

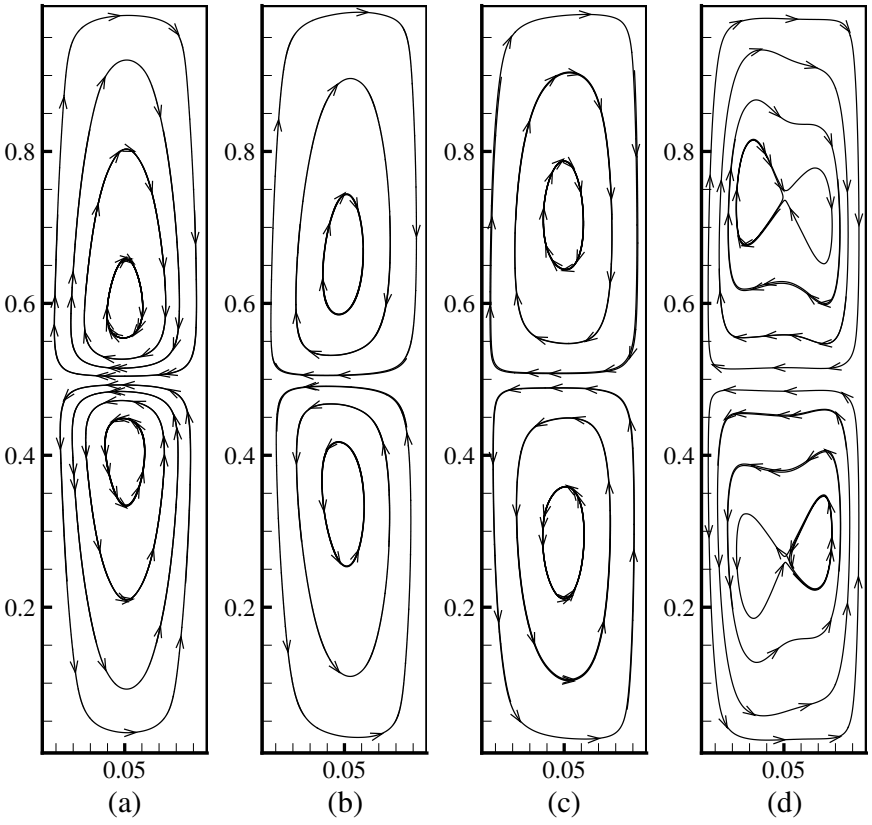

Figure 8. Streamlines inside the cavity for different magnetic Rayleigh numbers: (a) $Ra_m = 10^6$ (b) $Ra_m = 10^7$ (c) $Ra_m = 10^8$ (d) $Ra_m = 10^9$.

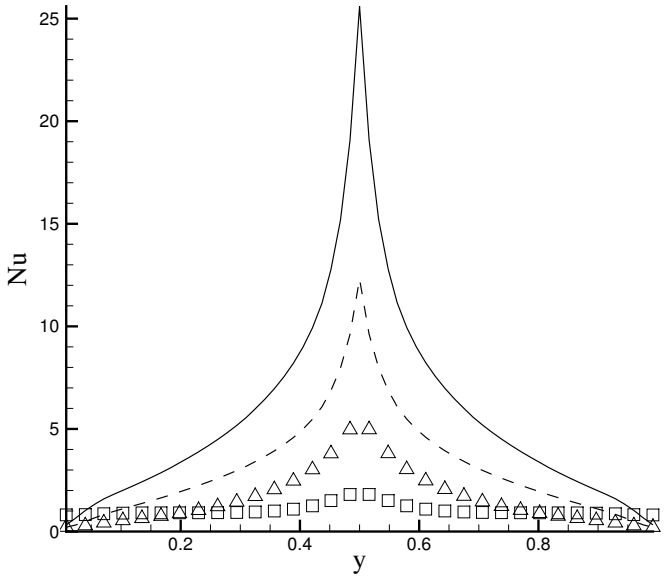

Figure 9. Local Nusselt number on the hot wall for different magnetic Rayleigh numbers: (a) $Ra_m = 10^6$ (b) $Ra_m = 10^7$ (c) $Ra_m = 10^8$ (d) $Ra_m = 10^9$.

5. ACKNOWLEDGEMENTS

The authors wish to acknowledge the support of this work by FAPESP-Brazil under the grant number 2017/05643-8 and by CNPq-Brazil under the grants 142376/2017-5.

6. REFERENCES

Ashouri, M., Ebrahimi, B., Shafii, M., Saidi, M. and Saidi, M., 2010. "Correlation for nusselt number in pure magnetic convection ferrofluid flow in a square cavity by a numerical investigation". *Journal of Magnetism and Magnetic Materials*, Vol. 322, No. 22, pp. 3607–3613.

Bessaih, R. and Kadja, M., 2000. "Turbulent natural convection cooling of electronic components mounted on a vertical channel". *Applied thermal engineering*, Vol. 20, No. 2, pp. 141–154.

Casula, M.F., Corrias, A., Arosio, P., Lascialfari, A., Sen, T., Floris, P. and Bruce, I.J., 2011. "Design of water-based ferrofluids as contrast agents for magnetic resonance imaging". *Journal of colloid and interface science*, Vol. 357, No. 1, pp. 50–55.

Cheng, H.C., Xu, S., Liu, Y., Levi, S. and Wu, S.T., 2011. "Adaptive mechanical-wetting lens actuated by ferrofluids". *Optics Communications*, Vol. 284, No. 8, pp. 2118–2121.

Cunha, F., Sobral, Y. and Gontijo, R., 2013. "Stabilization of concentration waves in fluidized beds of magnetic particles". *Powder technology*, Vol. 241, pp. 219–229.

Cunha, F.R., Couto, H. and Marcelino, N., 2007. "A study on magnetic convection in a narrow rectangular cavity". *Magnetohydrodynamics*, Vol. 43, No. 4, pp. 421–428.

de Vahl Davis, G., 1983. "Natural convection of air in a square cavity: a bench mark numerical solution". *International Journal for numerical methods in fluids*, Vol. 3, No. 3, pp. 249–264.

Fossa, M., Ménézo, C. and Leonardi, E., 2008. "Experimental natural convection on vertical surfaces for building integrated photovoltaic (bipv) applications". *Experimental Thermal and Fluid Science*, Vol. 32, No. 4, pp. 980–990.

Ghadiri, M., Sardarabadi, M., Pasandideh-fard, M. and Moghadam, A.J., 2015. "Experimental investigation of a pvt system performance using nano ferrofluids". *Energy Conversion and Management*, Vol. 103, pp. 468–476.

Harlow, F.H. and Welch, J.E., 1965. "Numerical calculation of time-dependent viscous incompressible flow of fluid with free surface". *The physics of fluids*, Vol. 8, No. 12, pp. 2182–2189.

Ivanov, A.O. and Kuznetsova, O.B., 2001. "Magnetic properties of dense ferrofluids: an influence of interparticle correlations". *Physical Review E*, Vol. 64, No. 4, p. 041405.

Katharina, D. and Kerstin, L.B., 2015. "Stability analysis of ferrofluids". *Current Directions in Biomedical Engineering*, Vol. 1, No. 1, pp. 10–13.

Kim, J. and Moin, P., 1985. "Application of a fractional-step method to incompressible navier-stokes equations". *Journal of computational physics*, Vol. 59, No. 2, pp. 308–323.

Kose, A.R., Fischer, B., Mao, L. and Koser, H., 2009. "Label-free cellular manipulation and sorting via biocompatible

ferrofluids". *Proceedings of the National Academy of Sciences*, Vol. 106, No. 51, pp. 21478–21483.

MacCaig, M., 1987. *Permanent magnets in theory and practice*. Pentech Press.

Odenbach, S. and Müller, H., 2005. "On the microscopic interpretation of the coupling of the symmetric velocity gradient to the magnetization relaxation". *Journal of magnetism and magnetic materials*, Vol. 289, pp. 242–245.

Ostrach, S., 1988. "Natural convection in enclosures". *Journal of Heat Transfer*, Vol. 110, No. 4b, pp. 1175–1190.

Oztop, H.F. and Abu-Nada, E., 2008. "Numerical study of natural convection in partially heated rectangular enclosures filled with nanofluids". *International journal of heat and fluid flow*, Vol. 29, No. 5, pp. 1326–1336.

Rosensweig, R.E., 2013. *Ferrohydrodynamics*. Courier Corporation.

Sheikholeslami, M. and Gorji-Bandpy, M., 2014. "Free convection of ferrofluid in a cavity heated from below in the presence of an external magnetic field". *Powder Technology*, Vol. 256, pp. 490–498.

Shliomis, M.I., 2001. "Ferrohydrodynamics: Testing a third magnetization equation". *Physical Review E*, Vol. 64, No. 6, p. 060501.

Viskanta, R., Kim, D. and Gau, C., 1986. "Three-dimensional natural convection heat transfer of a liquid metal in a cavity". *International journal of heat and mass transfer*, Vol. 29, No. 3, pp. 475–485.

Zitek, P. and Valenta, V., 2014. "Solution of heat removal from nuclear reactors by natural convection". In *EPJ Web of Conferences*. EDP Sciences, Vol. 67, p. 02133.

7. RESPONSIBILITY NOTICE

The authors are the only responsible for the printed material included in this paper.